Determination of the quark coupling strength /V$_{ub}$/ using baryonic decays

LHCb Collaboration; Aaij, R.; Adeva, B.; Adinolfi, M.; Affolder, A.; Ajaltouni, Z.; Akar, S.; Albrecht, J.; Alessio, F.; Alexander, M.; Ali, S.; Alkhazov, G.; Cartelle, P. Alvarez; Alves, A. A.; Amato, S.; Amerio, S.; Amhis, Y.; An, L.; Anderlini, L.; Anderson, J.

[Link to publication on Research at Birmingham portal](#)

Determination of the quark coupling strength |V_{ub}| using baryonic decays

The LHCb collaboration[†]

In the Standard Model of particle physics, the strength of the couplings of the *b* quark to the *u* and *c* quarks, |V_{ub}| and |V_{cb}|, are governed by the coupling of the quarks to the Higgs boson. Using data from the LHCb experiment at the Large Hadron Collider, the probability for the Λ_b^0 baryon to decay into the $p\mu^-\overline{\nu}_\mu$ final state relative to the $\Lambda_c^+\mu^-\overline{\nu}_\mu$ final state is measured. Combined with theoretical calculations of the strong interaction and a previously measured value of |V_{cb}|, the first |V_{ub}| measurement to use a baryonic decay is performed. This measurement is consistent with previous determinations of |V_{ub}| using *B* meson decays to specific final states and confirms the existing incompatibility with those using an inclusive sample of final states.

In the Standard Model (SM) of particle physics, the decay of one quark to another by the emission of a virtual *W* boson is described by the 3 × 3 unitary Cabibbo–Kobayashi–Maskawa (CKM) matrix[1,2]. This matrix arises from the coupling of the quarks to the Higgs boson. Although the SM does not predict the values of the four free parameters of the CKM matrix, the measurements of these parameters in different processes should be consistent with each other. If they are not, it is a sign of physics beyond the SM. In global fits combining all available measurements[3,4], the sensitivity of the overall consistency check is limited by the precision in the measurements of the magnitude and phase of the matrix element V_{ub}, which describes the transition of a *b* quark to a *u* quark.

The magnitude of V_{ub} can be measured via the semileptonic quark-level transition $b \to u\ell^-\overline{\nu}_\ell$. Semileptonic decays are used to minimize the uncertainties arising from the interaction of the strong force, described by quantum chromodynamics (QCD), between the final-state quarks. For the measurement of the magnitude of V_{ub}, as opposed to measurements of the phase, all decays of the *b* quark, and the equivalent $\overline{b}$ quark, can be considered together. There are two complementary methods to perform the measurement. From an experimental point of view, the simplest is to measure the branching fraction (probability to decay to a given final state) of a specific (exclusive) decay. An example is the decay of a $\overline{B}^0$ ($b\overline{d}$) meson to the final state $\pi^+\ell^-\overline{\nu}$, where the influence of the strong interaction on the decay, encompassed by a $\overline{B}^0 \to \pi^+$ form factor, is predicted by non-perturbative techniques such as lattice QCD (LQCD; ref. 5) or QCD sum rules[6]. The world average from ref. 7 for this method, using the decays $\overline{B}^0 \to \pi^+\ell^-\overline{\nu}$ and $B^- \to \pi^0\ell^-\overline{\nu}$, is |$V_{ub}$| = $(3.28 \pm 0.29) \times 10^{-3}$, where the most precise experimental inputs come from the BaBar[8,9] and Belle[10,11] experiments. The uncertainty is dominated by the LQCD calculations, which have recently been updated[12,13] and result in larger values of V_{ub} than the average given in ref. 7. The alternative method is to measure the differential decay rate in an inclusive way over all possible *B* meson decays containing the $b \to u\ell^-\overline{\nu}$ quark-level transition. This results in |V_{ub}| = $(4.41 \pm 0.15^{+0.15}_{-0.17}) \times 10^{-3}$ (ref. 14), where the first uncertainty arises from the experimental measurement and the second from theoretical calculations. The discrepancy between the exclusive and inclusive |V_{ub}| determinations is approximately three standard deviations and has been a long-standing puzzle in flavour physics. Several explanations have been proposed, such as

the presence of a right-handed (vector plus axial-vector) coupling as an extension of the SM beyond the left-handed (vector minus axial-vector) *W* coupling[15–18]. A similar discrepancy also exists between exclusive and inclusive measurements of |V_{cb}| (the coupling of the *b* quark to the *c* quark)[14].

This article describes a measurement of the ratio of branching fractions of the Λ_b^0 (*bud*) baryon into the $p\ell^-\overline{\nu}$ and $\Lambda_c^+\ell^-\overline{\nu}$ final states. This is performed using proton–proton collision data from the LHCb detector, corresponding to 2.0 fb^{-1} of integrated luminosity collected at a centre-of-mass energy of 8 TeV. The $b \to u$ transition, $\Lambda_b^0 \to p\mu^-\overline{\nu}_\mu$, has not been considered before as Λ_b^0 baryons are not produced at an e^+e^- *B*-factory; however, at the LHC, they constitute around 20% of the *b*-hadrons produced[19]. These measurements together with recent LQCD calculations[20] allow for the determination of |V_{ub}|^2/|V_{cb}|^2 according to

$$\frac{|V_{ub}|^2}{|V_{cb}|^2} = \frac{\mathcal{B}(\Lambda_b^0 \to p\mu^-\overline{\nu}_\mu)}{\mathcal{B}(\Lambda_b^0 \to \Lambda_c^+\mu^-\overline{\nu}_\mu)} R_{FF} \quad (1)$$

where $\mathcal{B}$ denotes the branching fraction and R_{FF} is a ratio of the relevant form factors, calculated using LQCD. This is then converted into a measurement of |V_{ub}| using the existing measurements of |V_{cb}| obtained from exclusive decays. The normalization to the $\Lambda_b^0 \to \Lambda_c^+\mu^-\overline{\nu}_\mu$ decay cancels many experimental uncertainties, including the uncertainty on the total production rate of Λ_b^0 baryons. At the LHC, the number of signal candidates is large, allowing the optimization of the event selection and the analysis approach to minimize systematic effects.

The LHCb detector[21,22] is one of the four major detectors at the Large Hadron Collider. It is instrumented in a cone around the proton beam axis, covering the angles between 10 and 250 mrad, where most *b*-hadron decays produced in proton–proton collisions occur. The detector includes a high-precision tracking system with a dipole magnet, providing a measurement of momentum and impact parameter (IP), defined for charged particles as the minimum distance of a track to a primary proton–proton interaction vertex (PV). Different types of charged particles are distinguished using information from two ring-imaging Cherenkov detectors, a calorimeter and a muon system. Simulated samples of specific signal and background decay modes of *b* hadrons are used at many stages throughout the analysis. These simulated events
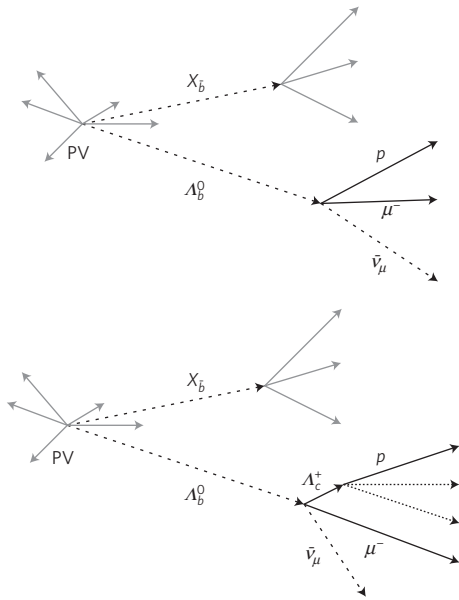
Figure 1 | Diagram illustrating the topology for the (top) signal and (bottom) background decays. The Λ_b^0 baryon travels about 1 cm on average before decaying; its flight direction is indicated in the diagram. In the $\Lambda_b^0 \to p\mu^-\overline{\nu}_\mu$ signal case, the only other particles present are typically reconstructed far away from the signal, which are shown as grey arrows. For the background from Λ_c^+ decays, there are particles that are reconstructed in close proximity to the signal, which are indicated as dotted arrows.

model the experimental conditions in full detail, including the proton–proton collision, the decay of the particles, and the response of the detector. The software used is described in refs 23–29.

Candidates of the signal modes are required to pass a trigger system[30] which reduces in real time the rate of recorded collisions (events) from the 40 MHz read-out clock of the LHC to around 4 kHz. For this analysis, the trigger requires a muon with a large momentum transverse to the beam axis that at the same time forms a good vertex with another track in the event. This vertex should be displaced from the PVs in the event. The identification efficiency for these high-momentum muons is 98%.

In the selection of the final states, stringent particle identification (PID) requirements are applied to the proton. These criteria are accompanied by a requirement that its momentum is greater than 15 GeV/c, as the PID performance is most effective for protons above the momentum threshold to produce Cherenkov light. The $p\mu^-$ vertex fit is required to be of good quality, which reduces background from most of the $b \to c\mu^-\overline{\nu}_\mu$ decays, as the resulting ground state charmed hadrons have significant lifetime.

To reconstruct $\Lambda_b^0 \to (\Lambda_c^+ \to pK^-\pi^+)\mu^-\overline{\nu}_\mu$ candidates, two additional tracks, positively identified as a pion and kaon, are combined with the proton to form a $\Lambda_c^+ \to pK^-\pi^+$ candidate. These are reconstructed from the same $p\mu^-$ vertex as the $\Lambda_b^0 \to p\mu^-\overline{\nu}_\mu$ signal to minimize systematic uncertainties. As the lifetime of the Λ_c^+ is short compared to other weakly decaying charm hadrons, the requirement has an acceptable efficiency.

There is a large background from b-hadron decays, with additional charged tracks in the decay products, as illustrated in Fig. 1. To reduce this background, a multivariate machine learning algorithm (a boosted decision tree, BDT (refs 31,32)) is employed to determine the compatibility of each track from a charged particle in the event to originate from the same vertex as the signal candidate. This isolation BDT includes variables such as the change in vertex quality if the track is combined with the signal vertex, as well as kinematic and IP information of the track that is tested. For

the BDT, the training sample of well-isolated tracks consists of all tracks apart from the signal decay products in a sample of simulated $\Lambda_b^0 \to p\mu^-\overline{\nu}_\mu$ events. The training sample of non-isolated tracks consists of the tracks from charged particles in the decay products X in a sample of simulated $\Lambda_b^0 \to (\Lambda_c^+ \to pX)\mu^-\overline{\nu}_\mu$ events. The BDT selection removes 90% of background with additional charged particles from the signal vertex, whereas it retains more than 80% of signal. The same isolation requirement is placed on both the $\Lambda_b^0 \to p\mu^-\overline{\nu}_\mu$ and $\Lambda_b^0 \to (\Lambda_c^+ \to pK^-\pi^+)\mu^-\overline{\nu}_\mu$ decay candidates, where the pion and kaon are ignored in the calculation of the BDT response for the $\Lambda_b^0 \to (\Lambda_c^+ \to pK^-\pi^+)\mu^-\overline{\nu}_\mu$ case.

The Λ_b^0 mass is reconstructed using the so-called corrected mass[33], defined as

$$m_{\mathrm{corr}} = \sqrt{m_{h\mu}^2 + p_\perp^2} + p_\perp$$

where $m_{h\mu}$ is the visible mass of the $h\mu$ pair and $p_\perp$ is the momentum of the $h\mu$ pair transverse to the Λ_b^0 flight direction, where h represents either the proton or Λ_c^+ candidate. The flight direction is measured using the PV and Λ_b^0 vertex positions. The uncertainties on the PV and the Λ_b^0 vertex are estimated for each candidate and propagated to the uncertainty on m_{corr}; the dominant contribution is from the uncertainty in the Λ_b^0 vertex.

Candidates with an uncertainty of less than 100 MeV/c^2 on the corrected mass are selected for the $\Lambda_b^0 \to p\mu^-\overline{\nu}_\mu$ decay. This selects only 23% of the signal; however, the separation between signal and background for these candidates is significantly improved and the selection thus reduces the dependence on background modelling.

The LQCD form factors that are required to calculate $|V_{ub}|$ are most precise in the kinematic region where q^2, the invariant mass squared of the muon and the neutrino in the decay, is high. The neutrino is not reconstructed, but q^2 can still be determined using the Λ_b^0 flight direction and the Λ_b^0 mass, but only up to a two-fold ambiguity. The correct solution has a resolution of about 1 GeV^2/c^4, whereas the wrong solution has a resolution of 4 GeV^2/c^4. To avoid influence on the measurement by the large uncertainty in form factors at low q^2, both solutions are required to exceed 15 GeV^2/c^4 for the $\Lambda_b^0 \to p\mu^-\overline{\nu}_\mu$ decay and 7 GeV^2/c^4 for the $\Lambda_b^0 \to (\Lambda_c^+ \to pK^-\pi^+)\mu^-\overline{\nu}_\mu$ decay. Simulation shows that only 2% of $\Lambda_b^0 \to p\mu^-\overline{\nu}_\mu$ decays and 5% of $\Lambda_b^0 \to \Lambda_c^+\mu^-\overline{\nu}_\mu$ decays with q^2 values below the cut values pass the selection requirements. The effect of this can be seen in Fig. 2, where the efficiency for the signal below 15 GeV^2/c^4 is reduced significantly if requirements are applied on both solutions. It is also possible that both solutions are imaginary owing to the limited detector resolution. Candidates of this type are rejected. The overall q^2 selection has an efficiency of 38% for $\Lambda_b^0 \to p\mu^-\overline{\nu}_\mu$ decays and 39% for $\Lambda_b^0 \to \Lambda_c^+\mu^-\overline{\nu}_\mu$ decays in their respective high-q^2 regions.

The mass distributions of the signal candidates for the two decays are shown in Fig. 3. The signal yields are determined from separate χ^2 fits to the m_{corr} distributions of the $\Lambda_b^0 \to p\mu^-\overline{\nu}_\mu$ and $\Lambda_b^0 \to (\Lambda_c^+ \to pK^-\pi^+)\mu^-\overline{\nu}_\mu$ candidates. The shapes of the signal and background components are modelled using simulation, where the uncertainties coming from the finite size of the simulated samples are propagated in the fits. The yields of all background components are allowed to vary within uncertainties obtained as described below.

For the fit to the m_{corr} distribution of the $\Lambda_b^0 \to p\mu^-\overline{\nu}_\mu$ candidates, many sources of background are accounted for. The largest of these is the cross-feed from $\Lambda_b^0 \to \Lambda_c^+\mu^-\overline{\nu}_\mu$ decays, where the Λ_c^+ decays into a proton and other particles that are not reconstructed. The amount of background arising from these decay modes is estimated by fully reconstructing two Λ_c^+ decays in the data. The background where the additional particles include charged particles originating directly from the Λ_c^+ decay is estimated by reconstructing $\Lambda_b^0 \to (\Lambda_c^+ \to pK^-\pi^+)\mu^-\overline{\nu}_\mu$ decays, whereas the
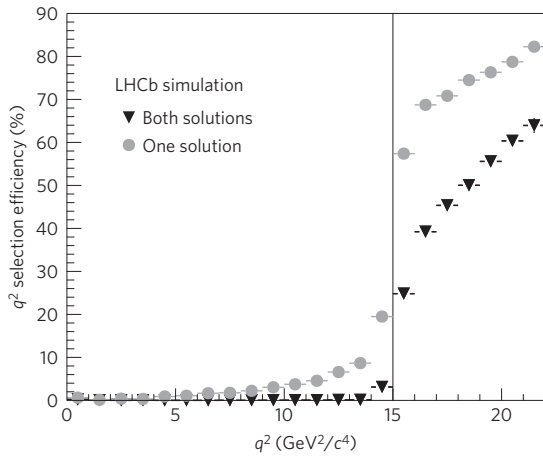
Figure 2 | Illustrating the method used to reduce the number of selected events from the q^2 region where lattice QCD has high uncertainties. The efficiency of simulated $\Lambda_b^0 \to p\mu^-\bar{\nu}_\mu$ candidates as a function of q^2. For the case where one q^2 solution is required to be above 15 GeV^2/c^4 (marked by the vertical line), there is still significant efficiency for the signal below this value, whereas, when both solutions have this requirement, only a small amount of signal below 15 GeV^2/c^4 is selected.

background where only neutral particles come directly from the Λ_c^+ decay is estimated by reconstructing $\Lambda_b^0 \to (\Lambda_c^+ \to pK_s^0)\mu^-\bar{\nu}_\mu$ decays. These two background categories are separated because the isolation BDT significantly reduces the charged component but has no effect on the neutral case. For the rest of the Λ_c^+ decay modes, the relative branching fraction between the decay and either the $\Lambda_c^+ \to pK^-\pi^+$ or $\Lambda_c^+ \to pK_s^0$ decay modes, as appropriate, is taken from ref. 14. For some neutral decay modes, where only the corresponding mode with charged decay particles is measured, assumptions based on isospin symmetry are used. In these decays, an uncertainty corresponding to 100% of the branching fraction is allowed for in the fit. Background from $\Lambda_b^0 \to D^0 p\mu^-\bar{\nu}_\mu$ decays is constrained in a similar way to the Λ_c^+ charged decay modes, with the normalization done relative to $\Lambda_b^0 \to D^0(\to K^-\pi^+)p\mu^-\bar{\nu}_\mu$ decays reconstructed in the data.

Any background with a Λ_c^+ baryon may also arise from decays of the type $\Lambda_b^0 \to (\Lambda_c^{*+} \to \Lambda_c^+\pi\pi)\mu^-\bar{\nu}_\mu$, where Λ_c^{*+} represents the $\Lambda_c(2595)^+$ or $\Lambda_c(2625)^+$ resonances as well as non-resonant contributions. The proportions between the $\Lambda_b^0 \to (\Lambda_c^{*+} \to \Lambda_c^+\pi\pi)\mu^-\bar{\nu}_\mu$ and the $\Lambda_b^0 \to \Lambda_c^+\mu^-\bar{\nu}_\mu$ backgrounds are determined from the fit to the $\Lambda_b^0 \to (\Lambda_c^+ \to pK^-\pi^+)\mu^-\bar{\nu}_\mu$ m_{corr} distribution and then used in the $\Lambda_b^0 \to p\mu^-\bar{\nu}_\mu$ fit.

The decays $\Lambda_b^0 \to N^*\mu^-\bar{\nu}_\mu$, where the N^* baryon decays into a proton and other non-reconstructed particles, are very similar to the signal decay and have poorly known branching fractions. The N^* resonance represents any of the states $N(1,440)$, $N(1,520)$, $N(1,535)$ or $N(1,770)$. None of the $\Lambda_b^0 \to N^*\mu^-\bar{\nu}_\mu$ decays have been observed and the m_{corr} shape of these decays is obtained using simulation samples generated according to the quark-model prediction of the form factors and branching fractions[34]. A 100% uncertainty is allowed for in the branching fractions of these decays.

Background where a pion or kaon is mis-identified as a proton originates from various sources and is measured by using a special data set where no PID is applied to the proton candidate. Finally, an estimate of combinatorial background, where the proton and muon originate from different decays, is obtained from a data set where the proton and muon have the same charge. The amount and shape of this background are in good agreement between the same-sign and opposite-sign $p\mu$ samples for corrected masses above 6 GeV/c^2.

For the $\Lambda_b^0 \to (\Lambda_c^+ \to pK^-\pi^+)\mu^-\bar{\nu}_\mu$ yield, the reconstructed $pK^-\pi^+$ mass is studied to determine the level of combinatorial

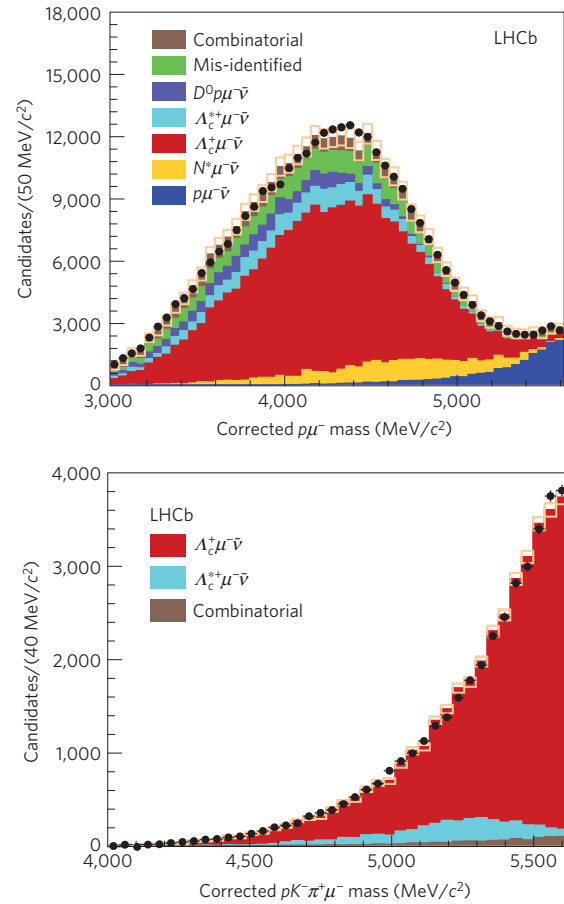**Figure 3 | Corrected mass fit used for determining signal yields.** Fits are made to (top) $\Lambda_b^0 \to p\mu^-\bar{\nu}_\mu$ and (bottom) $\Lambda_b^0 \to (\Lambda_c^+ \to pK^-\pi^+)\mu^-\bar{\nu}_\mu$ candidates. The statistical uncertainties arising from the finite size of the simulation samples used to model the mass shapes are indicated by open boxes and the data are represented by the black points. The statistical uncertainty on the data points is smaller than the marker size used. The different signal and background components appear in the same order in the fits and the legends. There are no data above the nominal Λ_b^0 mass owing to the removal of unphysical q^2 solutions.

background. The Λ_c^+ signal shape is modelled using a Gaussian function with an asymmetric power-law tail, and the background is modelled as an exponential function. Within a selected signal region of 30 MeV/c^2 from the known Λ_c^+ mass, the combinatorial background is 2% of the signal yield. Subsequently, a fit is performed to the m_{corr} distribution for $\Lambda_b^0 \to (\Lambda_c^+ \to pK^-\pi^+)\mu^-\bar{\nu}_\mu$ candidates, as shown in Fig. 3, which is used to discriminate between $\Lambda_b^0 \to \Lambda_c^+\mu^-\bar{\nu}_\mu$ and $\Lambda_b^0 \to (\Lambda_c^{*+} \to \Lambda_c^+\pi\pi)\mu^-\bar{\nu}_\mu$ decays.

The $\Lambda_b^0 \to p\mu^-\bar{\nu}_\mu$ and $\Lambda_b^0 \to (\Lambda_c^+ \to pK^-\pi^+)\mu^-\bar{\nu}_\mu$ yields are $17{,}687 \pm 733$ and $34{,}255 \pm 571$, respectively. This is the first observation of the decay $\Lambda_b^0 \to p\mu^-\bar{\nu}_\mu$.

The $\Lambda_b^0 \to p\mu^-\bar{\nu}_\mu$ branching fraction is measured relative to the $\Lambda_b^0 \to (\Lambda_c^+ \to pK^-\pi^+)\mu^-\bar{\nu}_\mu$ branching fraction. The relative efficiencies for reconstruction, trigger and final event selection are obtained from simulated events, with several corrections applied to improve the agreement between the data and the simulation. These correct for differences between data and simulation in the detector response and differences in the Λ_b^0 kinematic properties for the selected $\Lambda_b^0 \to p\mu^-\bar{\nu}_\mu$ and $\Lambda_b^0 \to (\Lambda_c^+ \to pK^-\pi^+)\mu^-\bar{\nu}_\mu$ candidates. The ratio of efficiencies is 3.52 ± 0.20, with the sources of the uncertainty described below.

Systematic uncertainties associated with the measurement are summarized in Table 1. The largest uncertainty originates from the

Table 1 | Summary of systematic uncertainties.

Source	Relative uncertainty (%)
$\mathcal{B}(\Lambda_c^+ \to pK^+\pi^-)$	$^{+4.7}_{-5.3}$
Trigger	3.2
Tracking	3.0
Λ_c^+ selection efficiency	3.0
$\Lambda_b^0 \to N^*\mu^-\bar{\nu}_\mu$ shapes	2.3
Λ_b^0 lifetime	1.5
Isolation	1.4
Form factor	1.0
Λ_b^0 kinematics	0.5
q^2 migration	0.4
PID	0.2
Total	$^{+7.8}_{-8.2}$

The table shows the relative systematic uncertainty on the ratio of the $\Lambda_b^0 \to p\mu^-\bar{\nu}_\mu$ and $\Lambda_b^0 \to \Lambda_c^+\mu^-\bar{\nu}_\mu$ branching fractions broken into its individual contributions. The total is obtained by adding them in quadrature. Uncertainties on the background levels are not listed here as they are incorporated into the fits.

Figure 4 | Experimental constraints on the left-handed coupling, $|V_{ub}^L|$ and the fractional right-handed coupling, ϵ_R. Whereas the overlap of the 68% confidence level bands for the inclusive[14] and exclusive[7] world averages of past measurements suggested a right-handed coupling of significant magnitude, the inclusion of the LHCb $|V_{ub}|$ measurement does not support this.

$\Lambda_c^+ \to pK^-\pi^+$ branching fraction, which is taken from ref. 35. This is followed by the uncertainty on the trigger response, which is due to the statistical uncertainty of the calibration sample. Other contributions come from the tracking efficiency, which is due to possible differences between the data and simulation in the probability of interactions with the material of the detector for the kaon and pion in the $\Lambda_b^0 \to (\Lambda_c^+ \to pK^-\pi^+)\mu^-\bar{\nu}_\mu$ decay. Another systematic uncertainty is assigned due to the limited knowledge of the momentum distribution for the $\Lambda_c^+ \to pK^-\pi^+$ decay products. Uncertainties related to the background composition are included in the statistical uncertainty for the signal yield through the use of nuisance parameters in the fit. The exception to this is the uncertainty on the $\Lambda_b^0 \to N^*\mu^-\bar{\nu}_\mu$ mass shapes due to the limited knowledge of the form factors and widths of each state, which is estimated by generating pseudoexperiments and assessing the impact on the signal yield.

Smaller uncertainties are assigned for the following effects: the uncertainty in the Λ_b^0 lifetime; differences in data and simulation in the isolation BDT response; differences in the relative efficiency and q^2 migration due to form factor uncertainties for both signal and normalization channels; corrections to the Λ_b^0 kinematic properties; the disagreement in the q^2 migration between data and simulation; and the finite size of the PID calibration samples. The total fractional systematic uncertainty is $^{+7.8}_{-8.2}$%, where the individual uncertainties are added in quadrature. The small impact of the form factor uncertainties means that the measured ratio of branching fractions can safely be considered independent of the theoretical input at the current level of precision.

From the ratio of yields and their determined efficiencies, the ratio of branching fractions of $\Lambda_b^0 \to p\mu^-\bar{\nu}_\mu$ to $\Lambda_b^0 \to \Lambda_c^+\mu^-\bar{\nu}_\mu$ in the selected q^2 regions is

$$\frac{\mathcal{B}(\Lambda_b^0 \to p\mu^-\bar{\nu}_\mu)_{q^2>15\,\text{GeV}/c^2}}{\mathcal{B}(\Lambda_b^0 \to \Lambda_c^+\mu^-\bar{\nu}_\mu)_{q^2>7\,\text{GeV}/c^2}} = (1.00 \pm 0.04 \pm 0.08) \times 10^{-2}$$

where the first uncertainty is statistical and the second is systematic. Using equation (1) with $R_{FF} = 0.68 \pm 0.07$, computed in ref. 20 for the restricted q^2 regions, the measurement

$$\frac{|V_{ub}|}{|V_{cb}|} = 0.083 \pm 0.004 \pm 0.004$$

is obtained. The first uncertainty arises from the experimental measurement and the second is due to the uncertainty in
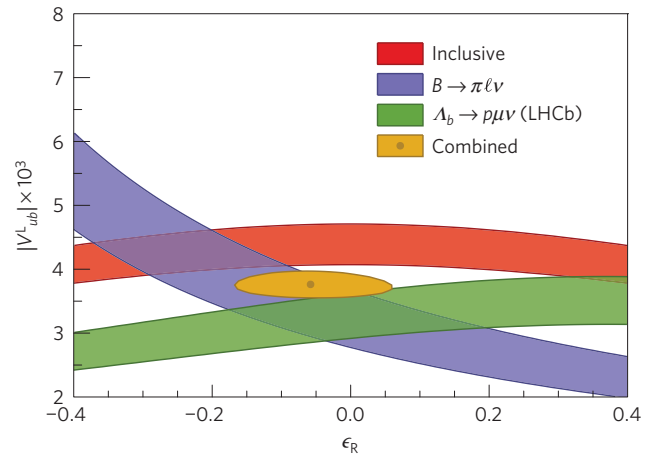
the LQCD prediction. Finally, using the world average $|V_{cb}| = (39.5 \pm 0.8) \times 10^{-3}$ measured using exclusive decays[14], $|V_{ub}|$ is measured as

$$|V_{ub}| = (3.27 \pm 0.15 \pm 0.16 \pm 0.06) \times 10^{-3}$$

where the first uncertainty is due to the experimental measurement, the second arises from the uncertainty in the LQCD prediction and the third from the normalization to $|V_{cb}|$. As the measurement of $|V_{ub}|/|V_{cb}|$ already depends on LQCD calculations of the form factors it makes sense to normalize to the $|V_{cb}|$ exclusive world average and not include the inclusive $|V_{cb}|$ measurements. The experimental uncertainty is dominated by systematic effects, most of which will be improved with additional data by a reduction of the statistical uncertainty of the control samples.

The measured ratio of branching fractions can be extrapolated to the full q^2 region using $|V_{cb}|$ and the form factor predictions[20], resulting in a measurement of $\mathcal{B}(\Lambda_b^0 \to p\mu^-\bar{\nu}_\mu) = (4.1 \pm 1.0) \times 10^{-4}$, where the uncertainty is dominated by knowledge of the form factors at low q^2.

The determination of $|V_{ub}|$ from the measured ratio of branching fractions depends on the size of a possible right-handed coupling[36]. This can clearly be seen in Fig. 4, which shows the experimental constraints on the left-handed coupling, $|V_{ub}^L|$, and the fractional right-handed coupling added to the SM, ϵ_R, for different measurements. The LHCb result presented here is compared to the world averages of the inclusive and exclusive measurements. Unlike the case for the pion in $\bar{B}^0 \to \pi^+\ell^-\bar{\nu}$ and $B^- \to \pi^0\ell^-\bar{\nu}$ decays, the spin of the proton is non-zero, allowing an axial-vector current, which gives a different sensitivity to ϵ_R. The overlap of the bands from the previous measurements suggested a significant right-handed coupling, but the inclusion of the LHCb $|V_{ub}|$ measurement does not support that.

In summary, a measurement of the ratio of $|V_{ub}|$ to $|V_{cb}|$ is performed using the exclusive decay modes $\Lambda_b^0 \to p\mu^-\bar{\nu}_\mu$ and $\Lambda_b^0 \to \Lambda_c^+\mu^-\bar{\nu}_\mu$. Using a previously measured value of $|V_{cb}|$, $|V_{ub}|$ is determined precisely. The $|V_{ub}|$ measurement is in agreement with the exclusively measured world average from ref. 7, but disagrees with the inclusive measurement[14] at a significance level of 3.5 standard deviations. The measurement will have a significant impact on the global fits to the parameters of the CKM matrix.

References

1. Cabibbo, N. Unitary symmetry and leptonic decays. *Phys. Rev. Lett.* **10**, 531–533 (1963)
2. Kobayashi, M. & Maskawa, T. CP violation in the renormalizable theory of weak interaction. *Prog. Theor. Phys.* **49**, 652–657 (1973)
3. Charles, J. *et al.* Current status of the Standard Model CKM fit and constraints on $\Delta F = 2$ New Physics. Preprint at http://arXiv.org/abs/1501.05013 (2015).
4. UTfit collaboration, Bona, M. *et al.* The Unitarity Triangle fit in the Standard Model and hadronic parameters from lattice QCD: A reappraisal after the measurements of Δm_s and $BR(B \to \tau \nu_\tau)$. *JHEP* **10**, 081 (2006); Preprint at http://arXiv.org/abs/hep-ph/0606167
5. Rothe, H. J. *Lattice Gauge Theories: An Introduction* 4th edn (World Scientific, 2012).
6. Dominguez, C. A. Introduction to QCD sum rules. *Mod. Phys. Lett. A* **28**, 1360002 (2013).
7. Heavy Flavor Averaging Group, Amhis, Y. *et al.* Averages of *b*-hadron, *c*-hadron, and τ-lepton properties as of summer 2014. Preprint at http://arXiv.org/abs/1412.7515 (2014).
8. BaBar collaboration, Lees, J. P. *et al.* Branching fraction and form-factor shape measurements of exclusive charmless semileptonic B decays, and determination of $|V_{ub}|$. *Phys. Rev. D* **86**, 092004 (2012).
9. BaBar collaboration, del Amo Sanchez, P. *et al.* Study of $B \to \pi \ell \nu$ and $B \to \rho \ell \nu$ decays and determination of $|V_{ub}|$. *Phys. Rev. D* **83**, 032007 (2011).
10. Belle collaboration, Ha, H. *et al.* Measurement of the decay $B^0 \to \pi^- \ell^+ \nu$ and determination of $|V_{ub}|$. *Phys. Rev. D* **83**, 071101 (2011).
11. Belle collaboration, Sibidanov, A. *et al.* Study of exclusive $B \to X_u \ell \nu$ decays and extraction of $|V_{ub}|$ using full reconstruction tagging at the Belle experiment. *Phys. Rev. D* **88**, 032005 (2013).
12. RBC and UKQCD collaborations, Flynn, J. M. *et al.* $B \to \pi \ell \nu$ and $B_s \to K \ell \nu$ form factors and $|V_{ub}|$ from 2+1-flavor lattice QCD with domain-wall light quarks and relativistic heavy quarks. *Phys. Rev. D* **91**, 074510 (2015).
13. Fermilab Lattice and MILC collaborations, Bailey, J. A. *et al.* $|V_{ub}|$ from $B \to \pi \ell \nu$ decays and $(2+1)$-flavor lattice QCD. Preprint at http://arXiv.org/abs/1503.07839 (2015).
14. Particle Data Group, Olive, K. A. *et al.* Review of particle physics. *Chin. Phys. C* **38**, 090001 (2014).
15. Chen, C.-H. & Nam, S.-h. Left-right mixing on leptonic and semileptonic $b \to u$ decays. *Phys. Lett. B* **666**, 462–466 (2008).
16. Crivellin, A. Effects of right-handed charged currents on the determinations of $|V_{ub}|$ and $|V_{cb}|$. *Phys. Rev. D* **81**, 031301 (2010).
17. Buras, A. J., Gemmler, K. & Isidori, G. Quark flavour mixing with right-handed currents: An effective theory approach. *Nucl. Phys. B* **843**, 107–142 (2011).
18. Crivellin, A. & Pokorski, S. Can the differences in the determinations of V_{ub} and V_{cb} be explained by New Physics? *Phys. Rev. Lett.* **114**, 011802 (2015).
19. LHCb collaboration, Aaij, R. *et al.* Measurement of *b* hadron production fractions in 7 TeV *pp* collisions. *Phys. Rev. D* **85**, 032008 (2012).
20. Detmold, W., Lehner, C. & Meinel, S. $\Lambda_b \to p \ell^- \bar{\nu}_\ell$ and $\Lambda_b \to \Lambda_c \ell^- \bar{\nu}_\ell$ form factors from lattice QCD with relativistic heavy quarks. Preprint at http://arXiv.org/abs/1503.01421 (2015).
21. LHCb collaboration, Alves, A. A. Jr *et al.* The LHCb detector at the LHC. *JINST* **3**, S08005 (2008).
22. LHCb collaboration, Aaij R. *et al.* LHCb detector performance. *Int. J. Mod. Phys. A* **30**, 1530022 (2015).
23. Sjöstrand, T., Mrenna, S. & Skands, P. PYTHIA 6.4 physics and manual. *JHEP* **05**, 026 (2006).
24. Belyaev, I. *et al.* Handling of the generation of primary events in Gauss, the LHCb simulation framework. *J. Phys. Conf. Ser.* **331**, 032047 (2011).
25. Lange, D. J. The EvtGen particle decay simulation package. *Nucl. Instrum. Methods A* **462**, 152–155 (2001).
26. Golonka, P. & Was, Z. PHOTOS Monte Carlo: A precision tool for QED corrections in *Z* and *W* decays. *Eur. Phys. J. C* **45**, 97–107 (2006).
27. Geant4 collaboration, Allison, J. *et al.* Geant4 developments and applications. *IEEE Trans. Nucl. Sci.* **53**, 270–278 (2006).
28. Geant4 collaboration, Agostinelli, S. *et al.* Geant4: A simulation toolkit. *Nucl. Instrum. Methods A* **506**, 250–303 (2003).
29. Clemencic, M. *et al.* The LHCb simulation application, Gauss: Design, evolution and experience. *J. Phys. Conf. Ser.* **331**, 032023 (2011).
30. Aaij, R. *et al.* The LHCb trigger and its performance in 2011. *JINST* **8**, P04022 (2013).
31. Breiman, L., Friedman, J. H., Olshen, R. A. & Stone, C. J. *Classification and Regression Trees* (Wadsworth International Group, 1984).
32. Schapire, R. E. & Freund, Y. A decision-theoretic generalization of on-line learning and an application to boosting. *J. Comput. Syst. Sci.* **55**, 119–139 (1997).
33. SLD collaboration, Abe K. *et al.* A measurement of R(b) using a vertex mass tag. *Phys. Rev. Lett.* **80**, 660–665 (1998).
34. Pervin, M., Roberts, W. & Capstick, S. Semileptonic decays of heavy Λ baryons in a quark model. *Phys. Rev. C* **72**, 035201 (2005).
35. Belle collaboration, Zupanc A. *et al.* Measurement of the branching fraction $\mathcal{B}(\Lambda_c^+ \to pK^-\pi^+)$. *Phys. Rev. Lett.* **113**, 042002 (2014).
36. Bernlochner, F. U., Ligeti, Z. & Turczyk, S. New ways to search for right-handed current in $B \to \rho \mu \bar{\nu}$ decay. *Phys. Rev. D* **90**, 094003 (2014).

Acknowledgements

Author contributions

All authors have contributed to the publication, being variously involved in the design and the construction of the detectors, in writing software, calibrating sub-systems, operating the detectors and acquiring data, and finally analysing the processed data.

Additional information

Reprints and permissions information is available online at www.nature.com/reprints. Correspondence and requests for materials should be addressed to U. Egede (u.egede@imperial.ac.uk).

Competing financial interests

The authors declare no competing financial interests.

The LHCb collaboration

R. Aaij[38], B. Adeva[37], M. Adinolfi[46], A. Affolder[52], Z. Ajaltouni[5], S. Akar[6], J. Albrecht[9], F. Alessio[38], M. Alexander[51], S. Ali[41], G. Alkhazov[30], P. Alvarez Cartelle[53], A. A. Alves Jr[57], S. Amato[2], S. Amerio[22], Y. Amhis[7], L. An[3], L. Anderlini[17,g], J. Anderson[40], M. Andreotti[16,f], J. E. Andrews[58], R. B. Appleby[54], O. Aquines Gutierrez[10], F. Archilli[38], A. Artamonov[35], M. Artuso[59], E. Aslanides[6], G. Auriemma[25,n], M. Baalouch[5], S. Bachmann[11], J. J. Back[48], A. Badalov[36], C. Baesso[60], W. Baldini[16,38], R. J. Barlow[54], C. Barschel[38], S. Barsuk[7], W. Barter[38], V. Batozskaya[28], V. Battista[39], A. Bay[39], L. Beaucourt[4], J. Beddow[51], F. Bedeschi[23], I. Bediaga[1], L. J. Bel[41], I. Belyaev[31], E. Ben-Haim[8], G. Bencivenni[18], S. Benson[38], J. Benton[46], A. Berezhnoy[32], R. Bernet[40], A. Bertolin[22], M.-O. Bettler[38], M. van Beuzekom[41], A. Bien[11], S. Bifani[45], T. Bird[54], A. Birnkraut[9], A. Bizzeti[17,i], T. Blake[48], F. Blanc[39], J. Blouw[10], S. Blusk[59], V. Bocci[25], A. Bondar[34], N. Bondar[30,38], W. Bonivento[15], S. Borghi[54], M. Borsato[7], T. J. V. Bowcock[52], E. Bowen[40], C. Bozzi[16], S. Braun[11], D. Brett[54], M. Britsch[10], T. Britton[59], J. Brodzicka[54], N. H. Brook[46], A. Bursche[40], J. Buytaert[38], S. Cadeddu[15], R. Calabrese[16,f], M. Calvi[20,k], M. Calvo Gomez[36,p], P. Campana[18], D. Campora Perez[38], L. Capriotti[54], A. Carbone[14,d], G. Carboni[24,l], R. Cardinale[19,j], A. Cardini[15], P. Carniti[20], L. Carson[50], K. Carvalho Akiba[2,38], R. Casanova Mohr[36], G. Casse[52], L. Cassina[20,k], L. Castillo Garcia[38], M. Cattaneo[38], Ch. Cauet[9], G. Cavallero[19], R. Cenci[23,t], M. Charles[8], Ph. Charpentier[38], M. Chefdeville[4], S. Chen[54], S.-F. Cheung[55], N. Chiapolini[40], M. Chrzaszcz[40,26], X. Cid Vidal[38], G. Ciezarek[41], P. E. L. Clarke[50], M. Clemencic[38], H. V. Cliff[47], J. Closier[38], V. Coco[38], J. Cogan[6], E. Cogneras[5], V. Cogoni[15,e], L. Cojocariu[29], G. Collazuol[22], P. Collins[38], A. Comerma-Montells[11], A. Contu[15,38], A. Cook[46], M. Coombes[46], S. Coquereau[8], G. Corti[38], M. Corvo[16,f], B. Couturier[38], G. A. Cowan[50], D. C. Craik[48], A. Crocombe[48], M. Cruz Torres[60], S. Cunliffe[53], R. Currie[53], C. D'Ambrosio[38], J. Dalseno[46], P. N. Y. David[41], A. Davis[57], K. De Bruyn[41], S. De Capua[54], M. De Cian[11], J. M. De Miranda[1], L. De Paula[2], W. De Silva[57], P. De Simone[18], C.-T. Dean[51], D. Decamp[4], M. Deckenhoff[9], L. Del Buono[8], N. Déléage[4], D. Derkach[55], O. Deschamps[5], F. Dettori[38], B. Dey[40], A. Di Canto[38], F. Di Ruscio[24], H. Dijkstra[38], S. Donleavy[52], F. Dordei[11], M. Dorigo[39], A. Dosil Suárez[37], D. Dossett[48], A. Dovbnya[43], K. Dreimanis[52], L. Dufour[41], G. Dujany[54], F. Dupertuis[39], P. Durante[38], R. Dzhelyadin[35], A. Dziurda[26], A. Dzyuba[30], S. Easo[49,38], U. Egede[53], V. Egorychev[31], S. Eidelman[34], S. Eisenhardt[50], U. Eitschberger[9], R. Ekelhof[9], L. Eklund[51], I. El Rifai[5], Ch. Elsasser[40], S. Ely[59], S. Esen[11], H. M. Evans[47], T. Evans[55], A. Falabella[14], C. Färber[11], C. Farinelli[41], N. Farley[45], S. Farry[52], R. Fay[52], D. Ferguson[50], V. Fernandez Albor[37], F. Ferrari[14], F. Ferreira Rodrigues[1], M. Ferro-Luzzi[38], S. Filippov[33], M. Fiore[16,38,f], M. Fiorini[16,f], M. Firlej[27], C. Fitzpatrick[39], T. Fiutowski[27], P. Fol[53], M. Fontana[10], F. Fontanelli[19,j], R. Forty[38], O. Francisco[2], M. Frank[38], C. Frei[38], M. Frosini[17], J. Fu[21], E. Furfaro[24,l], A. Gallas Torreira[37], D. Galli[14,d], S. Gallorini[22,38], S. Gambetta[19,j], M. Gandelman[2], P. Gandini[55], Y. Gao[3], J. García Pardiñas[37], J. Garofoli[59], J. Garra Tico[47], L. Garrido[36], D. Gascon[36], C. Gaspar[38], U. Gastaldi[16], R. Gauld[55], L. Gavardi[9], G. Gazzoni[5], A. Geraci[21,v], D. Gerick[11], E. Gersabeck[11], M. Gersabeck[54], T. Gershon[48], Ph. Ghez[4], A. Gianelle[22], S. Gianì[39], V. Gibson[47], L. Giubega[29], V. V. Gligorov[38], C. Göbel[60], D. Golubkov[31], A. Golutvin[53,31,38], A. Gomes[1,a], C. Gotti[20,k], M. Grabalosa Gándara[5], R. Graciani Diaz[36], L. A. Granado Cardoso[38], E. Graugés[36], E. Graverini[40], G. Graziani[17], A. Grecu[29], E. Greening[55], S. Gregson[47], P. Griffith[45], L. Grillo[11], O. Grünberg[63], B. Gui[59], E. Gushchin[33], Yu. Guz[35,38], T. Gys[38], C. Hadjivasiliou[59], G. Haefeli[39], C. Haen[38], S. C. Haines[47], S. Hall[53], B. Hamilton[58], T. Hampson[46], X. Han[11], S. Hansmann-Menzemer[11], N. Harnew[55], S. T. Harnew[46], J. Harrison[54], J. He[38], T. Head[39], V. Heijne[41], K. Hennessy[52], P. Henrard[5], L. Henry[8], J. A. Hernando Morata[37], E. van Herwijnen[38], M. Heß[63], A. Hicheur[2], D. Hill[55], M. Hoballah[5], C. Hombach[54], W. Hulsbergen[41], T. Humair[53], N. Hussain[55], D. Hutchcroft[52], D. Hynds[51], M. Idzik[27], P. Ilten[56], R. Jacobsson[38], A. Jaeger[11], J. Jalocha[55], E. Jans[41], A. Jawahery[58], F. Jing[3], M. John[55], D. Johnson[38], C. R. Jones[47], C. Joram[38], B. Jost[38], N. Jurik[59], S. Kandybei[43], W. Kanso[6], M. Karacson[38], T. M. Karbach[38], S. Karodia[51], M. Kelsey[59], I. R. Kenyon[45], M. Kenzie[38], T. Ketel[42], B. Khanji[20,38,k], C. Khurewathanakul[39], S. Klaver[54], K. Klimaszewski[28], O. Kochebina[7], M. Kolpin[11], I. Komarov[39], R. F. Koopman[42], P. Koppenburg[41,38], M. Korolev[32], L. Kravchuk[33], K. Kreplin[11], M. Kreps[48], G. Krocker[11], P. Krokovny[34], F. Kruse[9], W. Kucewicz[26,o], M. Kucharczyk[26], V. Kudryavtsev[34], K. Kurek[28], T. Kvaratskheliya[31], V. N. La Thi[39], D. Lacarrere[38], G. Lafferty[54], A. Lai[15], D. Lambert[50], R. W. Lambert[42], G. Lanfranchi[18], C. Langenbruch[48], B. Langhans[38], T. Latham[48], C. Lazzeroni[45], R. Le Gac[6], J. van Leerdam[41], J.-P. Lees[4], R. Lefèvre[5], A. Leflat[32], J. Lefrançois[7], O. Leroy[6], T. Lesiak[26], B. Leverington[11], Y. Li[7], T. Likhomanenko[65,64], M. Liles[52], R. Lindner[38], C. Linn[38], F. Lionetto[40], B. Liu[15], S. Lohn[38], I. Longstaff[51], J. H. Lopes[2], P. Lowdon[40], D. Lucchesi[22,r], H. Luo[50], A. Lupato[22], E. Luppi[16,f], O. Lupton[55], F. Machefert[7], F. Maciuc[29], O. Maev[30], K. Maguire[54], S. Malde[55], A. Malinin[64], G. Manca[15,e], G. Mancinelli[6], P. Manning[59], A. Mapelli[38], J. Maratas[5], J. F. Marchand[4], U. Marconi[14], C. Marin Benito[36], P. Marino[23,38,t], R. Märki[39], J. Marks[11], G. Martellotti[25], M. Martinelli[39], D. Martinez Santos[42], F. Martinez Vidal[66], D. Martins Tostes[2], A. Massafferri[1], R. Matev[38], A. Mathad[48], Z. Mathe[38], C. Matteuzzi[20], A. Mauri[40], B. Maurin[39], A. Mazurov[45], M. McCann[53], J. McCarthy[45], A. McNab[54], R. McNulty[12], B. Meadows[57], F. Meier[9], M. Meissner[11], M. Merk[41], D. A. Milanes[62], M.-N. Minard[4], D. S. Mitzel[11], J. Molina Rodriguez[60], S. Monteil[5], M. Morandin[22], P. Morawski[27], A. Mordà[6], M. J. Morello[23,t], J. Moron[27], A.-B. Morris[50], R. Mountain[59], F. Muheim[50], J. Müller[9], K. Müller[40], V. Müller[9], M. Mussini[14], B. Muster[39], P. Naik[46], T. Nakada[39], R. Nandakumar[49], I. Nasteva[2], M. Needham[50], N. Neri[21], S. Neubert[11], N. Neufeld[38], M. Neuner[11], A. D. Nguyen[39], T. D. Nguyen[39], C. Nguyen-Mau[39,q], V. Niess[5], R. Niet[9], N. Nikitin[32], T. Nikodem[11], D. Ninci[23], A. Novoselov[35], D. P. O'Hanlon[48], A. Oblakowska-Mucha[27], V. Obraztsov[35], S. Ogilvy[51], O. Okhrimenko[44], R. Oldeman[15,e], C. J. G. Onderwater[67], B. Osorio Rodrigues[1], J. M. Otalora Goicochea[2], A. Otto[38], P. Owen[53], A. Oyanguren[66], A. Palano[13,c], F. Palombo[21,u], M. Palutan[18], J. Panman[38], A. Papanestis[49], M. Pappagallo[51], L. L. Pappalardo[16,f], C. Parkes[54], G. Passaleva[17], G. D. Patel[52], M. Patel[53], C. Patrignani[19,j], A. Pearce[54,49], A. Pellegrino[41], G. Penso[25,m], M. Pepe Altarelli[38],

S. Perazzini[14,d], P. Perret[5], L. Pescatore[45], K. Petridis[46], A. Petrolini[19,j], M. Petruzzo[21], E. Picatoste Olloqui[36], B. Pietrzyk[4], T. Pilař[48], D. Pinci[25], A. Pistone[19], S. Playfer[50], M. Plo Casasus[37], T. Poikela[38], F. Polci[8], A. Poluektov[48,34], I. Polyakov[31], E. Polycarpo[2], A. Popov[35], D. Popov[10], B. Popovici[29], C. Potterat[2], E. Price[46], J. D. Price[52], J. Prisciandaro[39], A. Pritchard[52], C. Prouve[46], V. Pugatch[44], A. Puig Navarro[39], G. Punzi[23,s], W. Qian[4], R. Quagliani[7,46], B. Rachwal[26], J. H. Rademacker[46], B. Rakotomiaramanana[39], M. Rama[23], M. S. Rangel[2], I. Raniuk[43], N. Rauschmayr[38], G. Raven[42], F. Redi[53], S. Reichert[54], M. M. Reid[48], A. C. dos Reis[1], S. Ricciardi[49], S. Richards[46], M. Rihl[38], K. Rinnert[52], V. Rives Molina[36], P. Robbe[7,38], A. B. Rodrigues[1], E. Rodrigues[54], J. A. Rodriguez Lopez[62], P. Rodriguez Perez[54], S. Roiser[38], V. Romanovsky[35], A. Romero Vidal[37], M. Rotondo[22], J. Rouvinet[39], T. Ruf[38], H. Ruiz[36], P. Ruiz Valls[66], J. J. Saborido Silva[37], N. Sagidova[30], P. Sail[51], B. Saitta[15,e], V. Salustino Guimaraes[2], C. Sanchez Mayordomo[66], B. Sanmartin Sedes[37], R. Santacesaria[25], C. Santamarina Rios[37], M. Santimaria[18], E. Santovetti[24,l], A. Sarti[18,m], C. Satriano[25,n], A. Satta[24], D. M. Saunders[46], D. Savrina[31,32], M. Schiller[38], H. Schindler[38], M. Schlupp[9], M. Schmelling[10], T. Schmelzer[9], B. Schmidt[38], O. Schneider[39], A. Schopper[38], M.-H. Schune[7], R. Schwemmer[38], B. Sciascia[18], A. Sciubba[25,m], A. Semennikov[31], I. Sepp[53], N. Serra[40], J. Serrano[6], L. Sestini[22], P. Seyfert[11], M. Shapkin[35], I. Shapoval[16,43,f], Y. Shcheglov[30], T. Shears[52], L. Shekhtman[34], V. Shevchenko[64], A. Shires[9], R. Silva Coutinho[48], G. Simi[22], M. Sirendi[47], N. Skidmore[46], I. Skillicorn[51], T. Skwarnicki[59], E. Smith[55,49], E. Smith[53], J. Smith[47], M. Smith[54], H. Snoek[41], M. D. Sokoloff[57,38], F. J. P. Soler[51], F. Soomro[39], D. Souza[46], B. Souza De Paula[2], B. Spaan[9], P. Spradlin[51], S. Sridharan[38], F. Stagni[38], M. Stahl[11], S. Stahl[38], O. Steinkamp[40], O. Stenyakin[35], F. Sterpka[59], S. Stevenson[55], S. Stoica[29], S. Stone[59], B. Storaci[40], S. Stracka[23,t], M. Straticiuc[29], U. Straumann[40], R. Stroili[22], L. Sun[57], W. Sutcliffe[53], K. Swientek[27], S. Swientek[9], V. Syropoulos[42], M. Szczekowski[28], P. Szczypka[39,38], T. Szumlak[27], S. T'Jampens[4], T. Tekampe[9], M. Teklishyn[7], G. Tellarini[16,f], F. Teubert[38], C. Thomas[55], E. Thomas[38], J. van Tilburg[41], V. Tisserand[4], M. Tobin[39], J. Todd[57], S. Tolk[42], L. Tomassetti[16,f], D. Tonelli[38], S. Topp-Joergensen[55], N. Torr[55], E. Tournefier[4], S. Tourneur[39], K. Trabelsi[39], M. T. Tran[39], M. Tresch[40], A. Trisovic[38], A. Tsaregorodtsev[6], P. Tsopelas[41], N. Tuning[41,38], A. Ukleja[28], A. Ustyuzhanin[65,64], U. Uwer[11], C. Vacca[15,e], V. Vagnoni[14], G. Valenti[14], A. Vallier[7], R. Vazquez Gomez[18], P. Vazquez Regueiro[37], C. Vázquez Sierra[37], S. Vecchi[16], J. J. Velthuis[46], M. Veltri[17,h], G. Veneziano[39], M. Vesterinen[11], J. V. Viana Barbosa[38], B. Viaud[7], D. Vieira[2], M. Vieites Diaz[37], X. Vilasis-Cardona[36,p], A. Vollhardt[40], D. Volyanskyy[10], D. Voong[46], A. Vorobyev[30], V. Vorobyev[34], C. Voß[63], J. A. de Vries[41], R. Waldi[63], C. Wallace[48], R. Wallace[12], J. Walsh[23], J. Wandernoth[11], J. Wang[59], D. R. Ward[47], N. K. Watson[45], D. Websdale[53], A. Weiden[40], M. Whitehead[48], D. Wiedner[11], G. Wilkinson[55,38], M. Wilkinson[59], M. Williams[38], M. P. Williams[45], M. Williams[56], F. F. Wilson[49], J. Wimberley[58], J. Wishahi[9], W. Wislicki[28], M. Witek[26], G. Wormser[7], S. A. Wotton[47], S. Wright[47], K. Wyllie[38], Y. Xie[61], Z. Xu[39], Z. Yang[3], X. Yuan[34], O. Yushchenko[35], M. Zangoli[14], M. Zavertyaev[10,b], L. Zhang[3], Y. Zhang[3], A. Zhelezov[11], A. Zhokhov[31], L. Zhong[3].

Primary affiliations

[1]Centro Brasileiro de Pesquisas Físicas (CBPF), Rio de Janeiro, Brazil. [2]Universidade Federal do Rio de Janeiro (UFRJ), Rio de Janeiro, Brazil. [3]Center for High Energy Physics, Tsinghua University, Beijing, China. [4]LAPP, Université Savoie Mont-Blanc, CNRS/IN2P3 Annecy-Le-Vieux, France. [5]Clermont Université, Université Blaise Pascal, CNRS/IN2P3, LPC, Clermont-Ferrand, France. [6]CPPM, Aix-Marseille Université, CNRS/IN2P3 Marseille, France. [7]LAL, Université Paris-Sud, CNRS/IN2P3 Orsay, France. [8]LPNHE, Université Pierre et Marie Curie, Université Paris Diderot, CNRS/IN2P3 Paris, France. [9]Fakultät Physik, Technische Universität Dortmund, Dortmund, Germany. [10]Max-Planck-Institut für Kernphysik (MPIK), Heidelberg, Germany. [11]Physikalisches Institut, Ruprecht-Karls-Universität Heidelberg, Heidelberg, Germany. [12]School of Physics, University College Dublin, Dublin, Ireland. [13]Sezione INFN di Bari, Bari, Italy. [14]Sezione INFN di Bologna, Bologna, Italy. [15]Sezione INFN di Cagliari, Cagliari, Italy. [16]Sezione INFN di Ferrara, Ferrara, Italy. [17]Sezione INFN di Firenze, Firenze, Italy. [18]Laboratori Nazionali dell'INFN di Frascati, Frascati, Italy. [19]Sezione INFN di Genova, Genova, Italy. [20]Sezione INFN di Milano Bicocca, Milano, Italy. [21]Sezione INFN di Milano, Milano, Italy. [22]Sezione INFN di Padova, Padova, Italy. [23]Sezione INFN di Pisa, Pisa, Italy. [24]Sezione INFN di Roma Tor Vergata, Roma, Italy. [25]Sezione INFN di Roma La Sapienza, Roma, Italy. [26]Henryk Niewodniczanski Institute of Nuclear Physics Polish Academy of Sciences, Kraków, Poland. [27]AGH - University of Science and Technology, Faculty of Physics and Applied Computer Science, Kraków, Poland. [28]National Center for Nuclear Research (NCBJ), Warsaw, Poland. [29]Horia Hulubei National Institute of Physics and Nuclear Engineering, Bucharest-Magurele, Romania. [30]Petersburg Nuclear Physics Institute (PNPI), Gatchina, Russia. [31]Institute of Theoretical and Experimental Physics (ITEP), Moscow, Russia. [32]Institute of Nuclear Physics, Moscow State University (SINP MSU), Moscow, Russia. [33]Institute for Nuclear Research of the Russian Academy of Sciences (INR RAN), Moscow, Russia. [34]Budker Institute of Nuclear Physics (SB RAS) and Novosibirsk State University, Novosibirsk, Russia. [35]Institute for High Energy Physics (IHEP), Protvino, Russia. [36]Universitat de Barcelona, Barcelona, Spain. [37]Universidad de Santiago de Compostela, Santiago de Compostela, Spain. [38]European Organization for Nuclear Research (CERN), Geneva, Switzerland. [39]Ecole Polytechnique Fédérale de Lausanne (EPFL), Lausanne, Switzerland. [40]Physik-Institut, Universität Zürich, Zürich, Switzerland. [41]Nikhef National Institute for Subatomic Physics, Amsterdam, The Netherlands. [42]Nikhef National Institute for Subatomic Physics and VU University Amsterdam, Amsterdam, The Netherlands. [43]NSC Kharkiv Institute of Physics and Technology (NSC KIPT), Kharkiv, Ukraine. [44]Institute for Nuclear Research of the National Academy of Sciences (KINR), Kyiv, Ukraine. [45]University of Birmingham, Birmingham, UK. [46]H.H. Wills Physics Laboratory, University of Bristol, Bristol, UK. [47]Cavendish Laboratory, University of Cambridge, Cambridge, UK. [48]Department of Physics, University of Warwick, Coventry, UK. [49]STFC Rutherford Appleton Laboratory, Didcot, UK. [50]School of Physics and Astronomy, University of Edinburgh, Edinburgh, UK. [51]School of Physics and Astronomy, University of Glasgow, Glasgow, UK. [52]Oliver Lodge Laboratory, University of Liverpool, Liverpool, UK. [53]Imperial College London, London, UK. [54]School of Physics and Astronomy, University of Manchester, Manchester, UK. [55]Department of Physics, University of Oxford, Oxford, UK. [56]Massachusetts Institute of Technology, Cambridge, Massachusetts, USA. [57]University of Cincinnati, Cincinnati, Ohio, USA. [58]University of Maryland, College Park, Maryland, USA. [59]Syracuse University, Syracuse, New York, USA. [60]Pontifícia Universidade Católica do Rio de Janeiro (PUC-Rio), Rio de Janeiro, Brazil, associated with 2. [61]Institute of Particle Physics, Central China Normal University, Wuhan, Hubei, China, associated with 3. [62]Departamento de Fisica, Universidad Nacional de Colombia, Bogota, Colombia, associated with 8. [63]Institut für Physik, Universität Rostock, Rostock, Germany, associated with 11. [64]National Research Centre Kurchatov Institute, Moscow, Russia, associated with 31. [65]Yandex School of Data Analysis, Moscow, Russia, associated with 31. [66]Instituto de Fisica Corpuscular (IFIC), Universitat de Valencia-CSIC, Valencia, Spain, associated with 36. [67]Van Swinderen Institute, University of Groningen, Groningen, The Netherlands, associated with 41.

Secondary affiliations

[a]Universidade Federal do Triângulo Mineiro (UFTM), Uberaba-MG, Brazil. [b]P.N. Lebedev Physical Institute, Russian Academy of Science (LPI RAS), Moscow, Russia. [c]Università di Bari, Bari, Italy. [d]Università di Bologna, Bologna, Italy. [e]Università di Cagliari, Cagliari, Italy. [f]Università di Ferrara, Ferrara, Italy. [g]Università di Firenze, Firenze, Italy. [h]Università di Urbino, Urbino, Italy. [i]Università di Modena e Reggio Emilia, Modena, Italy. [j]Università di Genova, Genova, Italy. [k]Università di Milano Bicocca, Milano, Italy. [l]Università di Roma Tor Vergata, Roma, Italy. [m]Università di Roma La Sapienza, Roma, Italy. [n]Università della Basilicata, Potenza, Italy. [o]AGH - University of Science and Technology, Faculty of Computer Science, Electronics and Telecommunications, Kraków, Poland. [p]LIFAELS, La Salle, Universitat Ramon Llull, Barcelona, Spain. [q]Hanoi University of Science, Hanoi, Viet Nam. [r]Università di Padova, Padova, Italy. [s]Università di Pisa, Pisa, Italy. [t]Scuola Normale Superiore, Pisa, Italy. [u]Università degli Studi di Milano, Milano, Italy. [v]Politecnico di Milano, Milano, Italy.